ADVANCED MATERIALS TECHNOLOGIES

Supporting Information

for *Adv. Mater. Technol.,* DOI: 10.1002/admt.202101043

Magnetically Activated Flexible Thermoelectric Switches Based on Interconnected Nanowire Networks

*Tristan da Câmara Santa Clara Gomes, Nicolas Marchal, Flavio Abreu Araujo, and Luc Piraux**

Supporting Information:

Magnetically activated flexible thermoelectric switches based on interconnected nanowire networks

*Tristan da Câmara Santa Clara Gomes, Nicolas Marchal, Flavio Abreu Araujo and Luc Piraux**

Institute of Condensed Matter and Nanosciences, Université catholique de Louvain, Place Croix du Sud 1, Louvain-la-Neuve, 1348, Belgium

S1 Magneto-thermoelectric properties of 3D multilayered nanowire networks

Figures S1a-b show the magnetic variation of the resistance R (a) and Seebeck coefficient S (b) measured by applying a magnetic field in the plane of a three-dimensional (3D) $Co_{50}Ni_{50}$/Cu crossed nanowire (CNW) network at room temperature (RT)[1]. It reveals similar magnetic dependencies of R and S, with similar amplitude (MR $= 1 - R_{\text{sat}}/R_0 \approx 30\%$,where R_0 and R_{sat} are the resistance for a external magnetic field $H = 0$ and at saturated magnetic field ($H = 7.5$ kOe), respectively, and MTP $= 1 - S_{\text{sat}}/S_0 \approx -34\%$, where S_0 and S_{sat} are the Seebeck coefficient for a external magnetic field $H = 0$ and at saturated magnetic field ($H = 7.5$ kOe), respectively. As seen in Figure S1b, the Seebeck coefficients S_0 and S_{sat} reach respectively about $-16.2\ \mu V/K$ and -21.7 μV/K, leading to $\Delta S = S_0 - S_{\text{sat}} =$ 5.5 μV/K.

Figures S1c-d show the magnetic variation of R (a) and S (b) measured by applying a magnetic field in the plane of a 3D Py/Cu CNW network at RT[2], where Py = $Ni_{80}Fe_{20}$. Here again, very similar magnetic dependencies of R and S are observed, with MR $\approx 17\%$ and MTP $\approx -25\%$. As seen in Figure S1d, the Seebeck coefficients S_0 and S_{sat} reach respectively about -19.7 μV/K and -24.8 μV/K, leading to $\Delta S = S_0 - S_{\text{sat}} =$ 5.1 μV/K.

Figure S2a shows the temperature variation of S_0 and S_{sat} for the $Co_{50}Ni_{50}$/Cu CNW network[1]. As seen, the Seebeck coefficients show linear temperature dependency in the temperature range investigated. Figure S2b shows the temperature variation of S_0 and S_{sat} for the Py/Cu CNW network[2]. As seen, the Seebeck coefficients show a slight saturation at temperatures around RT, contrasting to the temperature variation of the $Co_{50}Ni_{50}$/Cu CNW network shown in Figure S2a.

This contrasting temperature variation of the Seebeck coefficient of $Co_{50}Ni_{50}$/Cu and Py/Cu CNW networks around RT explains the different temperature variation observed for their respective thermocouple devices (see Figures 2c-d). Notably, the saturation of the Seebeck coefficient around RT for the Py/Cu leads to an increasing negative slope for the Seebeck coefficient of the Py/Cu - Co_xNi_{1-x} thermocouples due to the linear decrease of the Seebeck coefficient of Co_xNi_{1-x} CNW networks (see Supplementary Information Section C for more details).

Figure S2c shows the temperature evolution of the MTP ratio for $Co_{50}Ni_{50}$/Cu and Py/Cu CNW networks[1,2]. As seen, $Co_{50}Ni_{50}$/Cu CNW networks show a small variation of the MTP effect with decreasing temperature. This contrasts with the Py/Cu CNW networks, where the MTP effect is found to increase with temperature variation in the temperature range considered. This explains the contrasting temperature dependencies of the difference between the ΔV values obtained at zero field and at saturation field for $Co_{50}Ni_{50}$/Cu - Co_xNi_{1-x} and Py/Cu - Co_xNi_{1-x} themocouples observed in Figure 2c and 2d, respectively.

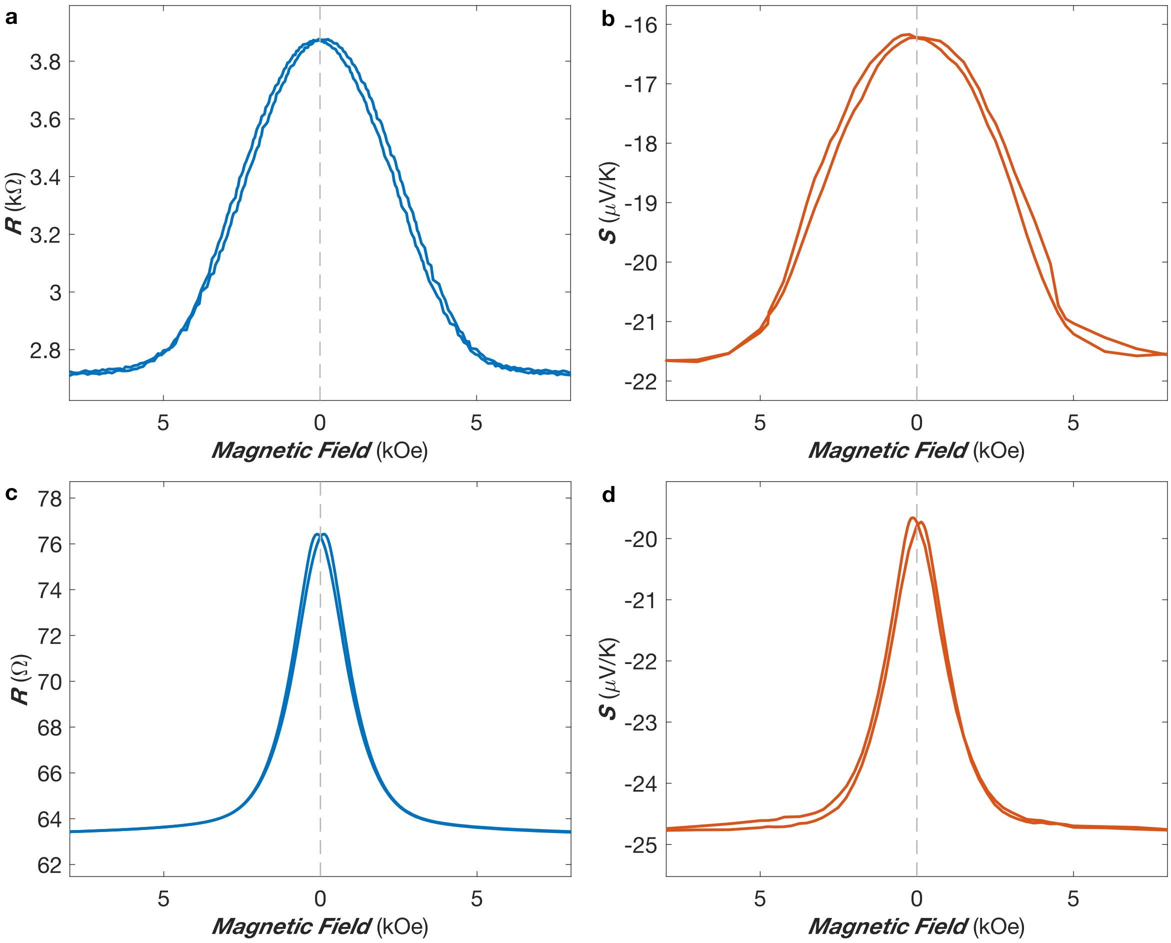

Figure S1: **Room temperature magnetic variation of the Resistance and Seebeck coefficient of 3D multilayer nanowire networks.** **a**, **b**, Magnetic variation of the resistance R (**a**) and Seebeck coefficient S (**b**) of 3D $Co_{50}Ni_{50}$/Cu crossed nanowire network at room temperature for an external magnetic field applied in the plane of the network. **c**, **d**, Magnetic variation of the resistance R (**c**) and Seebeck coefficient S (**d**) of 3D Py/Cu crossed nanowire network at room temperature for an external magnetic field applied in the plane of the network.

S2 Magneto-thermoelectric properties of homogeneous - multilayer thermocouples

For a homogeneous - multilayer CNWs thermocouples, the measured voltage ΔV of the NW-based thermocouple generated by a temperature gradient ΔT is given by

$$\Delta V = \int_{T_0}^{T_0+\Delta T} (S_{\mathrm{HM}}(T) - S_{\mathrm{ML}}(T))\,\mathrm{d}T, \tag{1}$$

where T_0 is the heat-sink base temperature and S_{HM} and S_{ML} are the Seebeck coefficients of the homogeneous CNWs and multilayer CNWs, respectively. When a magnetic field that saturates the FM layers of the multilayer CNWs is applied, the S_{ML} varies (as shown in Figs S1b and S1d), while the Seebeck coefficient of the homogeneous CNW shows marginal variation. Assuming small ΔT, this leads to a variation of the ΔV with the magnetic field that corresponds to about $\Delta S_{\mathrm{ML}}\Delta T$ with $\Delta S_{\mathrm{ML}} = S_{\mathrm{ML,\,0}} - S_{\mathrm{ML,\,sat}}$, where $S_{\mathrm{ML,\,0}}$ and $S_{\mathrm{ML,\,sat}}$ are the multilayer CNWs thermopower at zero-field and saturation.

$Co_{50}Ni_{50}$/Cu and Py/Cu multilayers have been selected as they display the largest ΔS_{ML} values among the multilayered CNWs previously investigated[1–4]. Table S1 shows the values of ΔS_{ML} for

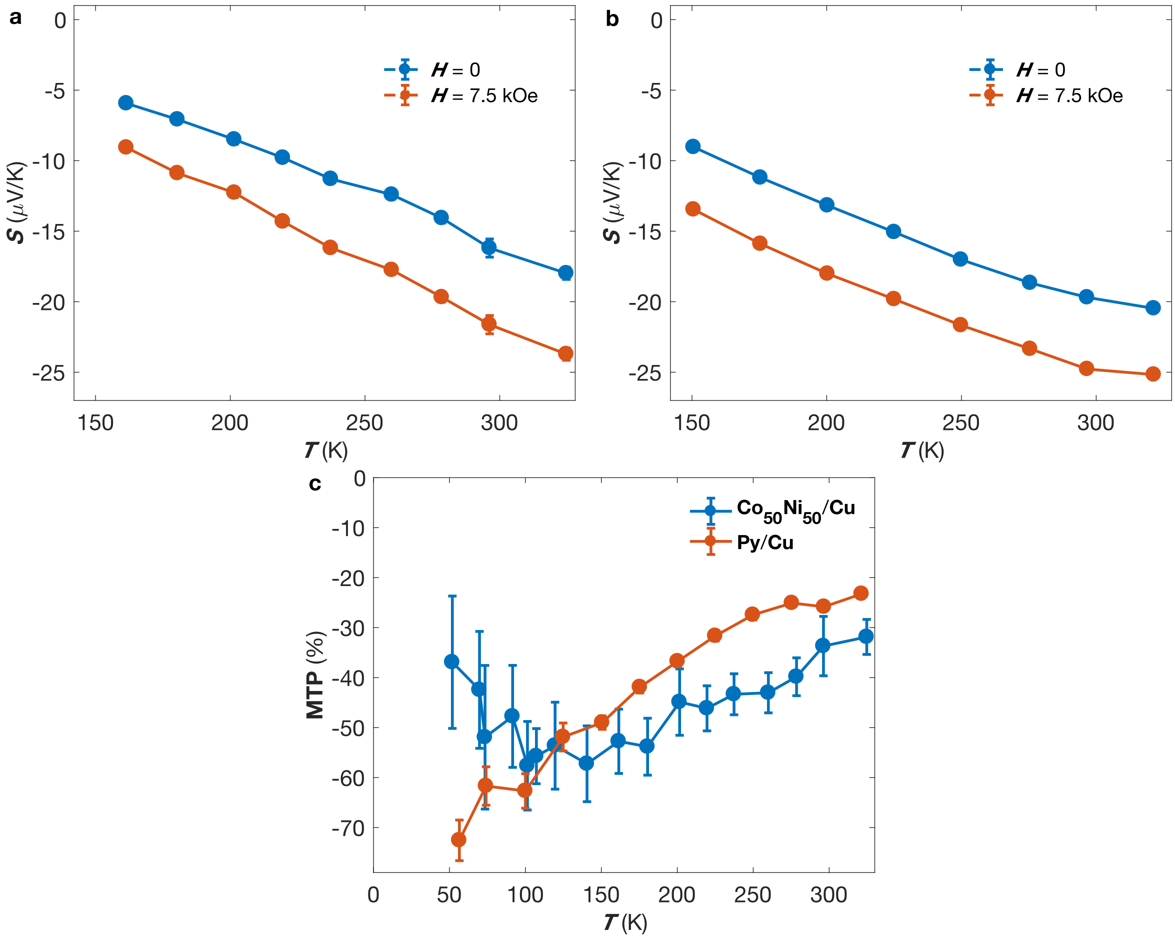

Figure S2: **Temperature dependencies of the Seebeck coefficient of 3D multilayer nanowire networks.** **a**, **b**, Seebeck coefficient S for a magnetic field $H = 0$ and 7.5 kOe applied in the plane of a 3D $Co_{50}Ni_{50}$/Cu (**a**) and a Py/Cu (**b**) crossed nanowire networks as a function of the temperature T. **c**, Temperature dependencies of the MTP ratio for the sample in (**a-b**). The error bars reflect the uncertainty of the voltage and temperature measurements and is set to two times the standard deviation, gathering 95% of the data variation.

several FM/Cu multilayered CNWs. Next, we selected CoNi alloys for the homogeneous CNWs as they allow to range from -20 μV/K (pure Ni) to -30 μV/K (pure Co), which are in the range to that of the Seebeck coefficient of $Co_{50}Ni_{50}$/Cu and Py/Cu CNWs at zero and saturation magnetic field. Moreover, it allows to select their Seebeck coefficient by simply adjusting the alloying composition, which have been found to be precisely controlled by fine-tuning the Ni^{2+} and Co^{2+} ions concentrations in the electrolyte[5,6].

Table S1: Variation of the Seebeck coefficient for an external magnetic field applied in the in-plane direction of various FM/Cu crossed nanowire networks.

FM/Cu CNWs	ΔS (μV/K)
Co/Cu	4.1
Ni/Cu	0.3
$Co_{50}Ni_{50}$/Cu	5.5
$Ni_{60}Ni_{40}$/Cu	2.0
Py/Cu	5.1
$Ni_{90}Ni_{10}$/Cu	4.0

The thermopower of a homogeneous - multilayer CNWs thermocouples $S(T) = S_{\mathrm{HM}}(T) -$

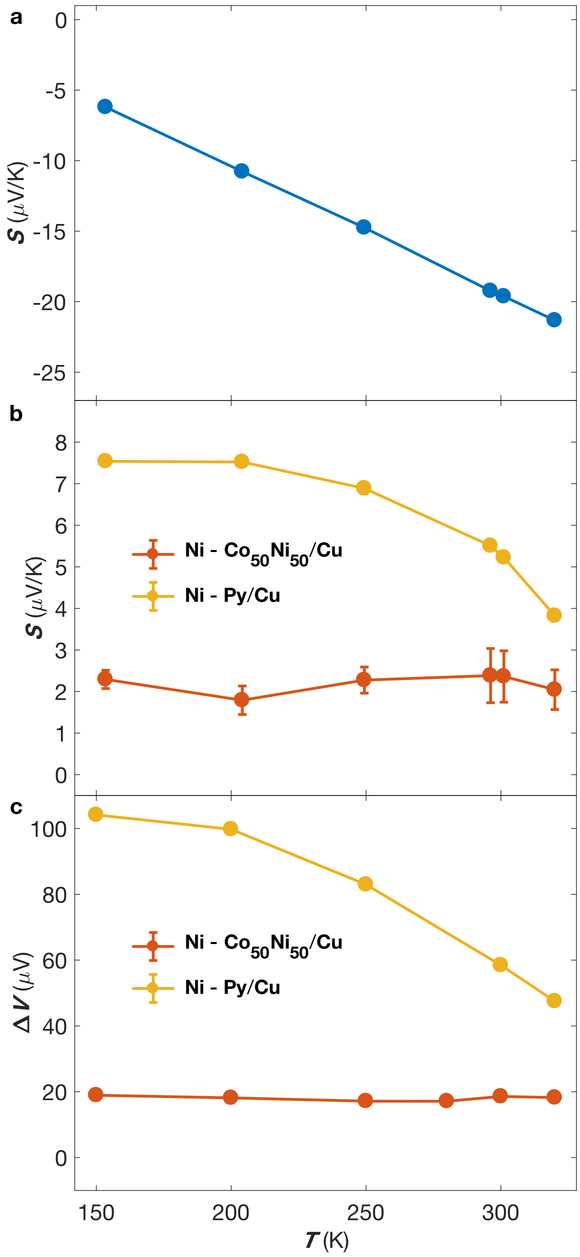

Figure S3: **Expected temperature variation of the thermocouples Seebeck coefficient.** **a**, Measured temperature variation of the Seebeck coefficient for a Ni nanowire network. **b**, Expected temperature variation of the saturated Seebeck coefficient $S(T) = S_{\rm HM}(T) - S_{\rm ML,\,sat}(T)$ for $Co_{50}Ni_{50}$/Cu - Ni (red curves) and Py/Cu - Ni (yellow curves) thermocouples using the data for the Ni nanowire network in (**a**) and the multilayer nanowire network from Figures S2a and S2b, respectively. **c**, Measured temperature dependence of the thermoelectric voltage ΔV obtained at $H = 7.5$ kOe for $\Delta T = 10$ K applied to $Co_{50}Ni_{50}$/Cu - Ni (red curves) and Py/Cu - Ni (yellow curves) thermocouples.

$S_{\rm ML}(T)$ can be estimated from the separated measurements performed on homogeneous CNWs and multilayer CNWs networks. Because the RT Seebeck coefficient of CoNi alloys CNW networks are found to be within -20 μV/K (pure Ni) and -30 μV/K (pure Co)[7], the RT thermopower of $Co_{50}Ni_{50}$/Cu - Co_xNi_{1-x} thermocouples can be expected to be found in the range of about $+2$ μV/K (pure Ni) and -8 μV/K (pure Co) at saturation (See the values for $S_{\rm ML}$ in Supplementary Section A). This corresponds well to the values of ΔV reported in Fig 2a for a temperature gradient $\Delta T = 10$ K applied to $Co_{50}Ni_{50}$/Cu - Co_xNi_{1-x} thermocouples at RT. Similarly, the expected RT thermopower of Py/Cu - Co_xNi_{1-x} thermocouples at saturation field are within about $+5$ μV/K (pure Ni) and -5 μV/K (pure Co), also in agreement with the results in Figure 2b.

As an example, Fig S3 shows the temperature variation expected and measured for the RT thermopower at saturation for $Co_{50}Ni_{50}$/Cu - Ni and Py/Cu - Ni thermocouples. The expected variations were estimated taking the temperature variation of the multilayer CNW networks in Figure S2 and the measured temperature variation of the Seebeck coefficient of a Ni CNW network (see Figure S3a)[7], which is mainly linear on the considered temperature range. As seen in Figure S3b, larger variation of the Seebeck coefficients are expected for the Py/Cu - Ni thermocouple, in particular around RT, because of the saturation observed for Py/Cu CNWs in Fig S2b. In contrast, the $Co_{50}Ni_{50}$/Cu - Ni thermocouple is expected to display only marginal variation with the temperature in the considered temperature range. The expected variation correspond well to the measured variation shown in Figure S3c, where the $Co_{50}Ni_{50}$/Cu - Ni sample showed almost unchanged thermoelectric output voltage ΔV (for $\Delta T = 10$ K) with the temperature in the range of 150 K to 320 K, while a pronounce decreased was obtained for the Py/Cu - Ni sample when the temperature increases from 150 K to 320 K. Similar observation were obtained for other CoNi alloying composition and explain the contrasting results in Figures 2c-d.

S3 Magnetoresistance properties of homogeneous - multilayer thermocouples

Figures S4a-b show the magnetic variation of the RT resistance R for $Co_{50}Ni_{50}$/Cu - Co_3Ni_{97} (a) and $Co_{50}Ni_{50}$/Cu - Ni (b) thermocouples, which correspond well to the magnetoresistance curve of $Co_{50}Ni_{50}$/Cu CNW networks (see Figure S1a). Moreover, the MR ratio reaches 27.5% and 27.7%, respectively, which is very close to the MR ratio recorded for $Co_{50}Ni_{50}$/Cu CNW networks ($\sim$30%, see Supplementary Information Section A). This is because the two thermoelectric legs are electrically connected in series and the resistance of the $Co_{50}Ni_{50}$/Cu CNW array (typically several hundred ohms to few kΩ, see Supplementary Information Section A) is significantly higher than that of the Co_3Ni_{97} CNW array (typically few ohms to few tens of ohms).

Figures S4c-d show the magnetic variation of the RT resistance R for Py/Cu - Co_3Ni_{97} (a) and Py/Cu - Ni (b) thermocouples. Once again, the shapes correspond well to that of Py/Cu CNW networks (see Figure S1c). For the Py/Cu - Co_xNi_{1-x} samples, the MR ratio were found to be smaller than that of Py/Cu ($\sim$17%, see Supplementary Information Section A). Indeed, the MR ratio values for the Py/Cu - Co_3Ni_{97} and Py/Cu - Ni thermocouples are 9.8% and 11.9%, respectively. This results from the fact that the resistance values of the Py/Cu CNW leg (typically a few tens of ohms, see Supplementary Information Section A) are close to that obtained for Co_3Ni_{97} CNW leg, the latter giving a very low MR signal.

Note that similar surface areas and deposition heights of CNWs were used for both legs of the thermocouple. A matching of the resistance and thermal conductance for the two thermocouple legs is possible by tuning the surface areas and deposition heights of the two different CNW networks.

S4 Experimental measurement uncertainty evaluation

The computation of the error bars is subject to the standard combination of the root-mean-square errors of the basic variables, here the tensions and the temperatures measured. Once the system reaches the steady-state, 200 tension or temperature measurements are taken to estimate the standard mean deviations (σ) of each measurements. Figure S5 shows the temperature (a) and voltage (b) measurements for the $Co_{50}Ni_{50}$/Cu - $Co_{53}Ni_{47}$ CNW network, which is representative of all the samples. In these measurements, the heater is turned on after 100 s, then the temperature and voltage settles during 600 s. The magnetic field is then turned on and the temperature and voltage settles during 600 s. The magnetic field and the heater are successively turned off, leaving always 600 s to ensure that the

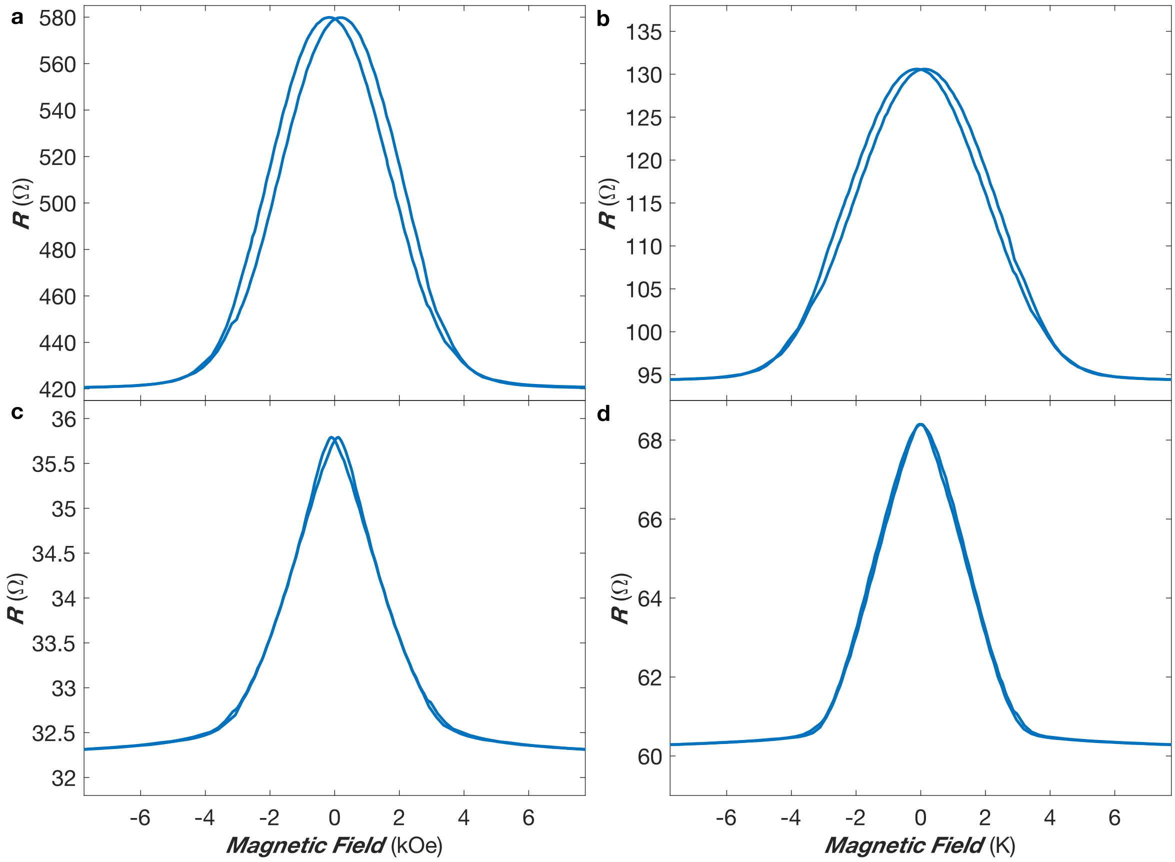

Figure S4: **Magnetoresistance curves of homogeneous - multilayer thermocouples.** **a**, **b**, **c**, **d**, Magnetic variation of the room-temperature resistance R for $Co_{50}Ni_{50}$/Cu - Co_3Ni_{97} (**a**), $Co_{50}Ni_{50}$/Cu - Ni (**b**), Py/Cu - Co_3Ni_{97} (**c**) and Py/Cu - Ni (**d**) thermocouples.

voltage and temperature reach steady-state.

The σ for T_0 and V_0 are taken as the standard deviation obtained for the 100 first measurements before turning on the resistive heater and the last 100 measurements after turning off the heater and reaching back the initial temperature. These measurements are indicated by the green areas in Figure S5. The σ for the temperature and voltage reached at $H = 0$ is taken as the standard deviation obtained for the last 100 measurements obtained before turning on the magnetic field and the last 100 measurements before turning off the heater, which are indicated by the blue areas in Figure S5. Finally, the σ for the temperature and voltage reached at a given magnetic field is taken as the standard deviation obtained for the last 200 measurements obtained before turning off the magnetic field shown as the red area in Figure S5. The error, or uncertainty, considered for these variables is set to 2 times σ (gathers 95% of the data variation) from the mean values. The rigorous combination of the different errors gives rise to the uncertainty of the parameters shown in our graphs.

The error over ΔT is then computed as:

$$\Delta T_{\text{err}} = \sqrt{T_{\text{err}}^2 + T_{0,\text{ err}}^2}, \tag{2}$$

where $T_{0,\text{ err}}$ and T_{err} are the errors of the base temperature T_0 and the temperature after turning on the heater. Similarly, the error over ΔV is then computed as:

$$\Delta V_{\text{err}} = \sqrt{V_{\text{err}}^2 + V_{0,\text{ err}}^2}, \tag{3}$$

where $V_{0,\text{ err}}$ and V_{err} are the errors of the base initial residual voltage V_0 and the steady-state voltage after turning on the heater (and the magnetic field for the error over ΔV at a given magnetic field).

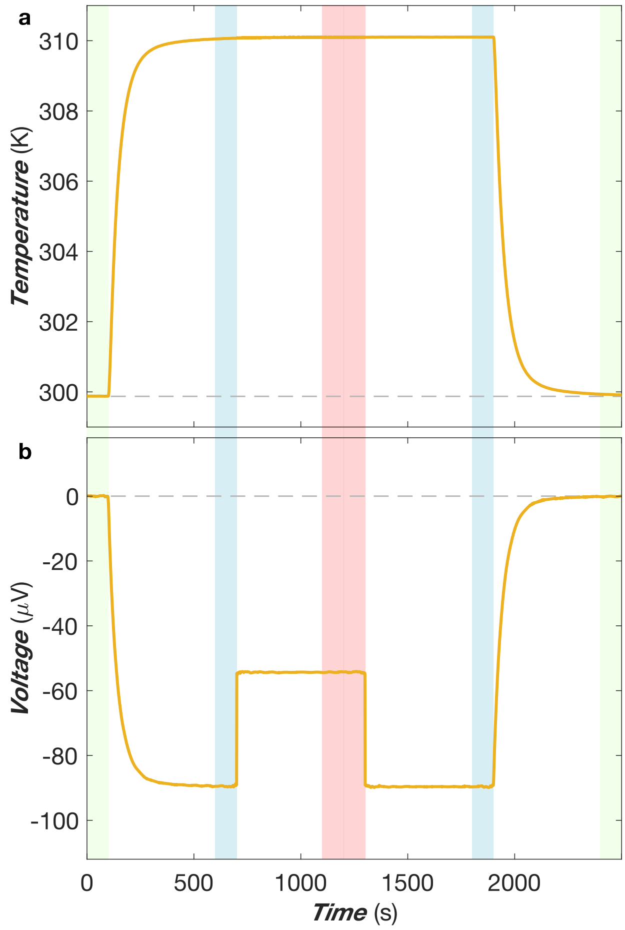

Figure S5: **Experimental measurement uncertainty evaluation.** **a**, **b**, Time dependence of the hot side temperature (**a**) and voltage differential ΔV at the thermocouple junction edge (**b**) for an interconnected $Co_{50}Ni_{50}$/Cu - $Co_{53}Ni_{47}$ nanowire network thermocouple at room temperature and $\Delta T = 10$ K. The heater is turned on after 100 s. The green, blue and red areas indicate the temperature and voltage used to estimate the standard mean deviations of the temperature and residual voltage before heating T_0 and V_0, the temperature T and voltage V at $H = 0$ and T and V at $H = 7.5$ kOe, respectively.

S5 Materials uncertainty evaluation

Other sources of error include variation in the Seebeck coefficient between samples of the same material, and the variation in material composition between samples. As the estimation of this error is more complex than that of experimental measurements, it has not been used for the error bars used in the figures. However, comparing the results obtained for $Co_{50}Ni_{50}$/Cu - Co_xNi_{1-x} and Py/Cu - Co_xNi_{1-x} CNW network thermocouples allows for an estimation of this error. Indeed, as only the multilayer network leg is modified, the variation of the ΔV for $\Delta T = 10$ K at RT as a function of the Co content x in the homogeneous network leg for the two kinds of thermocouples is expected to be the same. This is shown in Figure S6a for $H = 7.5$ kOe (we choose to compare the samples at saturation as this state is more comparable, in contrast, the zero magnetic field state might change more between samples as it also depends on the degree of anti-parallelism between FM layers magnetisations).

As seen in Figure S6a, the Co content dependencies of the voltage differential ΔV between the $Co_{50}Ni_{50}$/Cu - Co_xNi_{1-x} and Py/Cu - Co_xNi_{1-x} samples show similar tendencies, as expected. However, some variation can be observed. Indeed, looking at the difference between the voltage differential for $Co_{50}Ni_{50}$/Cu - Co_xNi_{1-x} and the voltage differential for Py/Cu - Co_xNi_{1-x} shown in Figure S6b (noted $\Delta V_{Co_{50}Ni_{50}/Cu} - \Delta V_{Py/Cu}$), it reveals a variation with the Co content x. The error related to

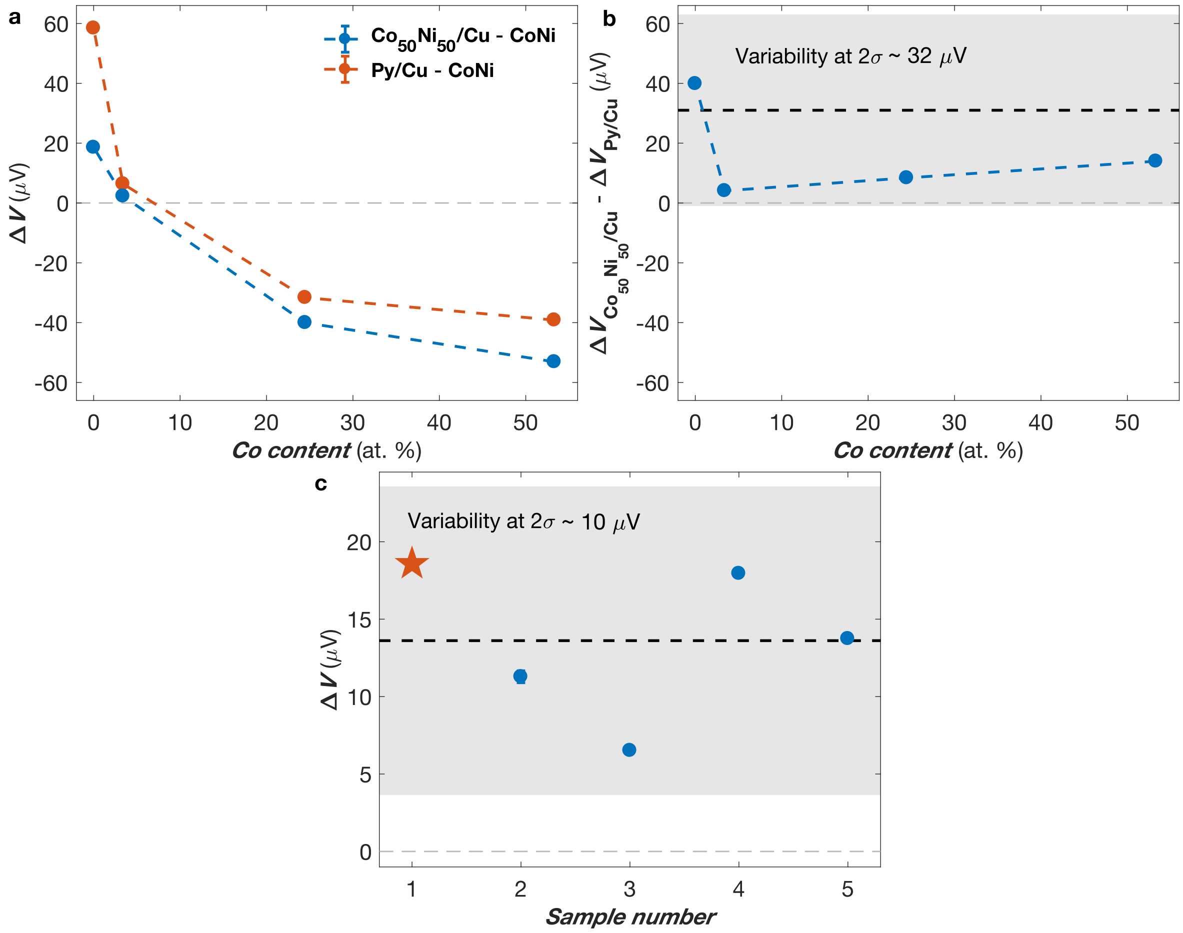

Figure S6: **Comparison between $Co_{50}Ni_{50}$/Cu and Py/Cu based samples. a**, Variation of the voltage differential ΔV recorded at the junction edges for a difference of temperature $\Delta T = 10$ K between the heat source and the heat sinks for $H = 7.5$ kOe as a function of the Co content x in the interconnected $Co_{50}Ni_{50}$/Cu - Co_xNi_{1-x} and Py/Cu - Co_xNi_{1-x} nanowire network thermocouples at room temperature. **b**, Difference between the voltage differential ΔV for $Co_{50}Ni_{50}$/Cu - Co_xNi_{1-x} and Py/Cu - Co_xNi_{1-x} nanowire network thermocouples in (**a**) as a function of the Co content x. The black dashed line corresponds to the difference between the room temperature Seebeck coefficient of $Co_{50}Ni_{50}$/Cu and Py/Cu in Figures S1b and S1d multiplied by $\Delta T = 10$ K. The grey area corresponds to the acceptable values around the dashed black line taking the error of 32 μV corresponding to 2 times the standard deviation of the data. **c**, Values of ΔV recorded for $\Delta T = 10$ K applied to five different $Co_{50}Ni_{50}$/Cu - Ni thermocouples showing the sample to sample variation. The red star indicates the sample used in Figure 2 and Figure 5. The grey area corresponds to the acceptable values around the mean value for the five samples (dashed black line) taking the error of 10 μV corresponding to 2 times the standard deviation of these five values.

sample to sample variation of the Seebeck coefficient has been estimated as two times the standard deviation of this variation, which gave an error of 32 μV for $\Delta T = 10$ K (i.e. an error of 3.2 μV/K). Please note that this error comes from lack of reproductibility between the Seebeck coefficient and variation of the alloying composition of four 3D CNW networks (the Py/Cu, $Co_{50}Ni_{50}$/Cu and two Co_xNi_{1-x} networks), which corresponds to about 0.8 μV/K per CNW network. This corresponds well to the typical sample to sample variation of the Seebeck coefficient of multilayer CNW networks of 1 μV/K that has been observed.

Taking the Seebeck coefficient of the $Co_{50}Ni_{50}$/Cu and Py/Cu samples at RT given in Supplementary information Section A, we can expect a variation of 3.1 μV/K between the $Co_{50}Ni_{50}$/Cu - Co_xNi_{1-x} and Py/Cu - Co_xNi_{1-x} samples (indicated by the black dashed line in S6b). Therefore, neglecting the temperature variation of their respective thermopowers, this induces an expected value for $\Delta V_{\text{Co}_{50}\text{Ni}_{50}\text{/Cu}} - \Delta V_{\text{Py/Cu}}$ of 31 μV for $\Delta T = 10$ K. As seen in Figure S6b, all experimental data lie within the shaded grey area that corresponds to this expected value and a variation of 32 μV around it. Furthermore, as the thermopowers of Py/Cu and $Co_{50}Ni_{50}$/Cu CNW networks tend to be closer as the temperature increases around RT (see Fig S3b), $\Delta V_{\text{Co}_{50}\text{Ni}_{50}\text{/Cu}} - \Delta V_{\text{Py/Cu}}$ is expected to e slightly smaller than 31 μV, in agreement with the results in Figure S6b.

The sample to sample variability has also been assessed by analysing the sample reproductibility. For this, we analyzed the results obtained for five different $Co_{50}Ni_{50}$/Cu - Ni thermocouples (the first sample being the one reported in Figures 2 and 5). Figure S6c shows the thermoelectric voltage at saturation recorded for the five samples at RT for $\Delta T = 10$ K. As indicated by the grey area, the data on the five samples gave a variability of about 10 μV. Note that this variation is reported for one thermocouple, in contrast to the one reported in Fig S6 that account for the variation of two compared thermocouples.

In contrast, the uncertainty at two σ related to measurement of a sample is typically less than 0.1 μV for a ΔT of 10 K (barely appearing in Figures S6b-c).

References

[1] T. da Câmara Santa Clara Gomes, F. Abreu Araujo, L. Piraux, *Science Advances* **2019**, *5*, 3 eaav2782.

[2] N. Marchal, T. da Câmara Santa Clara Gomes, F. Abreu Araujo, L. Piraux, *Nanoscale Research Letters* **2020**, *15*, 1 137.

[3] F. Abreu Araujo, T. da Câmara Santa Clara Gomes, L. Piraux, *Advanced Electronic Materials* **2019**, *5*, 8 1800819.

[4] N. Marchal, T. da Câmara Santa Clara Gomes, F. Abreu Araujo, L. Piraux, *Nanomaterials* **2021**, *11*, 5.

[5] T. da Câmara Santa Clara Gomes, J. De La Torre Medina, M. Lemaitre, L. Piraux, *Nanoscale Research Letters* **2016**, *11*, 1 466.

[6] T. da Câmara Santa Clara Gomes, N. Marchal, F. Abreu Araujo, Y. Velázquez Galván, J. de la Torre Medina, L. Piraux, *Nanomaterials* **2021**, *11*, 1.

[7] T. da Câmara Santa Clara Gomes, N. Marchal, F. Abreu Araujo, L. Piraux, *Nanomaterials* **2020**, *10*, 11.